Physica A 698 (2026) 131772

Contents lists available at ScienceDirect

Physica A

journal homepage: www.elsevier.com/locate/physa

Feedbacks between community lockdowns and vaccination incentives in epidemic dynamics

Shaojun Dang [a], Xiaoqian Zhao [a], Marko Gosak [b,c,d], Kaipeng Hu [a,*], Matjaž Perc [b,e,f,g,**]

[a] School of Statistics and Mathematics, Yunnan University of Finance and Economics, Kunming, 650221, People's Republic of China
[b] Faculty of Natural Sciences and Mathematics, University of Maribor, Koroška cesta 160, 2000 Maribor, Slovenia
[c] Faculty of Medicine, University of Maribor, Taborska ul. 8, 2000 Maribor, Slovenia
[d] Alma Mater Europaea University, Slovenska ulica 17, 2000 Maribor, Slovenia
[e] Community Healthcare Center Dr. Adolf Drolc Maribor, Ulica talcev 9, 2000 Maribor, Slovenia
[f] Department of Physics, Kyung Hee University, 26 Kyungheedae-ro, Seoul 02447, Republic of Korea
[g] University College, Korea University, 145 Anam-ro, Seoul 02841, Republic of Korea

ARTICLE INFO

Keywords:
Epidemic spread
Vaccination dilemma
Hyperbolic networks
Evolutionary game

ABSTRACT

We study the coevolution of epidemic spreading and voluntary vaccination under community lockdown on hyperbolic networks. By coupling an SIR process with an evolutionary vaccination game, we analyze how mobility restrictions interact with behavioral adaptation in structured populations. The effect of lockdown is found to vary with vaccination cost. For low vaccination cost, uptake remains high and lockdown has little additional influence. At intermediate cost, lockdown reduces perceived infection risk and suppresses vaccination, which can counterintuitively increase the final epidemic size despite lower transmissibility, a counterintuitive regime that is specific to high vaccine efficacy. For high vaccination cost, lockdown becomes the dominant control mechanism and substantially mitigates outbreaks, although it does not eliminate them. Lockdown also qualitatively alters the spreading dynamics, replacing synchronized global outbreaks with fragmented and asynchronous local waves. In addition, we identify a crossover in social cost that signals a transition from vaccination-dominated protection to transmission-limited control. These results show that interventions that suppress transmission may simultaneously weaken vaccination incentives through behavioral feedback.

1. Introduction

A large body of empirical evidence has shown that real-world social systems are characterized by heterogeneous degree distributions, high clustering, and pronounced community organization [1–6]. These structural properties play a fundamental role in the dynamics of the epidemic, influencing the thresholds of outbreak, the speed of spread, and the final size of the epidemic [7,8]. In particular, community structures partition populations into densely connected groups with relatively sparse external interactions, providing a natural basis for localized transmission and control of epidemics at the community-level [9]. However, the influence of social networks is not limited to the dynamics of disease transmission; it also profoundly shapes individual behavioral patterns

* Corresponding author.
** Corresponding author at: Faculty of Natural Sciences and Mathematics, University of Maribor, Koroška cesta 160, 2000 Maribor, Slovenia.
E-mail addresses: hu.kp1993@hotmail.com (K. Hu), matjaz.perc@gmail.com (M. Perc).

https://doi.org/10.1016/j.physa.2026.131772
Received 9 April 2026; Received in revised form 10 June 2026
Available online 18 June 2026

and decision-making mechanisms. In complex networks, individuals do not exist in isolation but are embedded in interdependent systems composed of social relationships. Therefore, people no longer pursue maximum benefit at minimum cost as in the traditional "economic man" assumption. Instead, due to extensive and complex connections with others, they often consider the well-being of others in the decision-making process, thus exhibiting behavioral characteristics similar to the "network man" [10,11]. This behavioral characteristic induced by the network structure is particularly prominent in the context of an epidemic. For example, people may take the initiative to self-isolate [12,13] or choose to get vaccinated [14]. Although these behaviors are usually accompanied by certain individual costs, they can effectively reduce the risk of infection for others. From this perspective, these behaviors essentially embody a cooperative mechanism [15–17]. Such large-scale cooperative behavior, even among non-relatives, is considered one of the important characteristics of human society.

In realistic epidemic settings, interventions are often implemented at the community level. Such measures do not necessarily imply complete closure or strict lockdown. More broadly, they can be understood as mechanisms that reduce effective cross-community contacts, including mobility restrictions, avoidance of high-risk areas, and improved protective attitudes when entering risky communities, such as mask wearing or disinfection [18–20]. These community-based restrictions suppress transmission by weakening inter-community spreading pathways. At the same time, they can also indirectly influence voluntary vaccination, because lower exposure to the risk of external infection can reduce the perceived benefit of vaccination [21,22]. Therefore, community-level intervention is important not only because it changes epidemic transmission routes but also because it reshapes the incentive structure that underlies vaccination decisions.

Voluntary vaccination has been extensively studied within the framework of evolutionary game theory, where individuals evaluate the trade-off between vaccination cost and infection risk under social interaction and information feedback [23–25]. Because vaccination decisions are adaptive and depend on epidemic conditions, the coupling between disease dynamics and strategic updating can generate insufficient vaccine uptake, recurrent outbreaks, and other complex dynamical outcomes [16,26–28]. However, most previous studies have focused on random, scale-free, or small-world networks [1,2,29], which do not explicitly represent geometric organization or controllable inter-community separation. As a consequence, they are limited in describing how reductions in cross-community interaction affect infection size and, in turn, alter vaccination incentives. To address this issue, we employ hyperbolic network models as a geometric framework to represent socially structured populations [30–32]. Previous work has shown that such networks provide a suitable setting to study the impact of community-level lockdown on epidemic spreading, revealing that reducing inter-community interactions alone may have limited effectiveness in suppressing global outbreaks [30]. However, these studies were conducted within a purely epidemiological framework, where individual behavior remained static and independent of epidemic conditions. In contrast, real-world epidemic dynamics are inherently shaped by adaptive behavioral responses. To capture this interplay, we extend the hyperbolic network framework by coupling epidemic spreading with an evolutionary vaccination game, thereby introducing a feedback loop between disease dynamics and individual decision-making. This allows us to investigate how transmission-reducing interventions may simultaneously alter behavioral incentives, potentially leading to emergent outcomes that cannot be inferred from epidemiological dynamics alone.

Motivated by these considerations, this paper investigates the coevolution of epidemic spreading and vaccination dynamics under community-based contact restrictions. We integrate an SIR epidemic process with an evolutionary vaccination game on hyperbolic random geometric networks [33]. Community lockdown is modeled as a reduction in cross-community transmission, while vaccination strategies are updated through payoff-driven stochastic imitation. Through systematic numerical simulations, we examine how the intensity of community-level contact restriction affects vaccination coverage and epidemic outcomes under different network structures.

Our results reveal a significant trade-off. While strengthened community lockdowns can effectively suppress large-scale outbreaks, this effect is accompanied by reduced vaccination mobilization. Consequently, we observed lower vaccination coverage and more complex outbreak patterns in these cases. These findings suggest that assessing the effectiveness of community-level interventions cannot be based solely on their direct epidemiological impacts but must also be understood in conjunction with their complex interactions with adaptive vaccination dynamics.

2. Model

We consider a model that integrates a coupled network structure, disease transmission dynamics, and individual behavior evolution to study the impact of community structure and lockdown measures on vaccination behavior and disease transmission. The model consists of three components: network generation, epidemic transmission, and evolutionary vaccination dynamics.

2.1. Network construction and community structure

We construct the contact network using a hyperbolic random geometric framework, which is known to naturally reproduce several structural properties commonly observed in real social networks, including heterogeneous degree distributions, high clustering, short average path lengths, and pronounced community structures [31,32,34–36].

Specifically, the nodes are embedded in a two-dimensional hyperbolic disk of radius $R_h = 12$. The growth of the network starts with an initial connected core of $n = 8$ nodes to ensure global connectivity. The new nodes are then introduced sequentially until the network size reaches $N = 5000$. Each node i is assigned polar coordinates (r_i, θ_i), where the radial coordinate r_i reflects the popularity of the node, while the angular coordinate θ_i represents similarity. Angular coordinates are drawn uniformly from $[0, 2\pi)$, while radial coordinates follow a growth-induced distribution.

$$\theta_i = 2\pi u_1 \tag{1}$$

$$r_i = \frac{1}{\alpha}\cosh^{-1}\left[1 + \cosh(\alpha R_h - 1)\, u_2\right] \tag{2}$$

Here α is the internal growth parameter, R_h is the radius of the hyperbolic disk, and u_1 and u_2 are random numbers sampled from a [0, 1] uniform distribution.

The probability of establishing a connection between two nodes depends on their hyperbolic distance, which decreases monotonically with distance. As a result, nodes that are closer in hyperbolic space are more likely to be connected.

$$d_{ij} = \cosh^{-1}\left[\cosh(r_i)\cosh(r_j) - \sinh(r_i)\sinh(r_j)\cos(\Delta\theta_{ij})\right] \tag{3}$$

where $\Delta\theta_{ij} = \pi - |\pi - |\theta_i - \theta_j||$ is the angular distance between node i and node j. In this geometric representation, the radial coordinate r_i reflects node popularity, with nodes closer to the center typically having higher degree, while the angular distance captures similarity, such that nodes with small angular separation can be interpreted as individuals that are socially or geographically proximate, for example belonging to the same region or socio-economic group.

To quantify community organization, we apply the Louvain modularity optimization algorithm [5,37].

$$Q = \frac{1}{2m}\sum_{i,j}^{N}\left[A_{ij} - \frac{k_i k_j}{2m}\right]\delta(c_i, c_j) \tag{4}$$

where m is the total number of edges in the network, A_{ij} is the adjacency matrix element that indicates whether there is an edge between node i and node j, k_i and k_j are the degrees of nodes i and j, and c_i and c_j are the communities to which nodes i and j belong, respectively and $\delta(c_i, c_j)$ is a delta function that is equal to 1 if $c_i = c_j$ and 0 otherwise. The algorithm continuously adjusts the community assignments of the nodes to maximize the modularity value Q. A higher modularity value indicates a more pronounced community structure in the network.

The resulting networks exhibit a modularity of $Q = 0.81$ and a clustering coefficient of $C = 0.65$, indicating a pronounced community structure and a high level of local clustering. These values are consistent with those reported in previous studies on complex networks with small-world and community properties [38]. Due to these genuine topological characteristics, the hyperbolic network model represents a viable platform to simulate various social phenomena, including epidemics [32,39–41]. Within this framework, the network construction and the implementation of community-level lockdown follow our previous work [30], providing a consistent baseline for incorporating adaptive vaccination dynamics.

2.2. Coevolutionary dynamics of vaccination and epidemic spreading

We consider a seasonal evolutionary framework in which vaccination behavior and epidemic spreading co-evolve across consecutive seasons, as illustrated in Fig. 1. Each season consists of two sequential phases: an epidemic spreading phase and a strategy updating phase. At the beginning of each season, individuals decide whether to vaccinate according to the strategy configuration inherited from the previous season. Once vaccination decisions are made, strategies remain fixed, and the epidemic spreads through the contact network under this static vaccination configuration. At the end of the epidemic season, individuals receive payoffs determined by their vaccination decisions and infection outcomes. Subsequently, individuals update their vaccination strategies through social learning based on the Fermi update rule: each individual compares their payoff with that of a randomly selected neighbor and adopts the neighbor's strategy with a probability increasing with the payoff difference. The updated strategy distribution then determines the initial vaccination configuration for the next season, thereby coupling behavioral adaptation with epidemic dynamics over time.

Specifically, at the beginning of each season, individuals decide whether to be vaccinated based on their experience in the previous season. For the initial season, a fraction $x_0 = 0.5$ of individuals is randomly selected to be vaccinated. We have verified that the qualitative results are robust with respect to the choice of initial conditions. After this initialization, the disease spreads on the network under a fixed vaccination configuration.

In the voluntary vaccination setting, vaccinated individuals incur a cost c, while unvaccinated individuals avoid this cost but face a risk of infection. We assume that vaccination provides complete immunity within each season, so vaccinated individuals do not participate in transmission. Unvaccinated individuals receive a payoff of -1 if infected and 0 otherwise. The vaccination cost is normalized relative to the infection loss, such that $c \in (0, 1)$.

To incorporate bounded rationality, we adopt an evolutionary updating rule. At the end of each season, individuals update their vaccination strategies based on accumulated payoffs. Strategy updating follows a local imitation process governed by the Fermi function [42–44]. Specifically, an individual i randomly selects a neighbor j and adopts j's strategy with probability

$$P_{i\leftarrow j} = \frac{1}{1 + \exp[\beta(\pi_i - \pi_j)]}. \tag{5}$$

where π_i and π_j denote the payoffs of individuals i and j, respectively, and β represents the selection intensity.

Disease spreading is modeled using a continuous-time Gillespie stochastic simulation [45,46]. Each individual can be in one of four states: susceptible (S), infected (I), recovered (R), or vaccinated (V). At the beginning of each season, vaccinated individuals

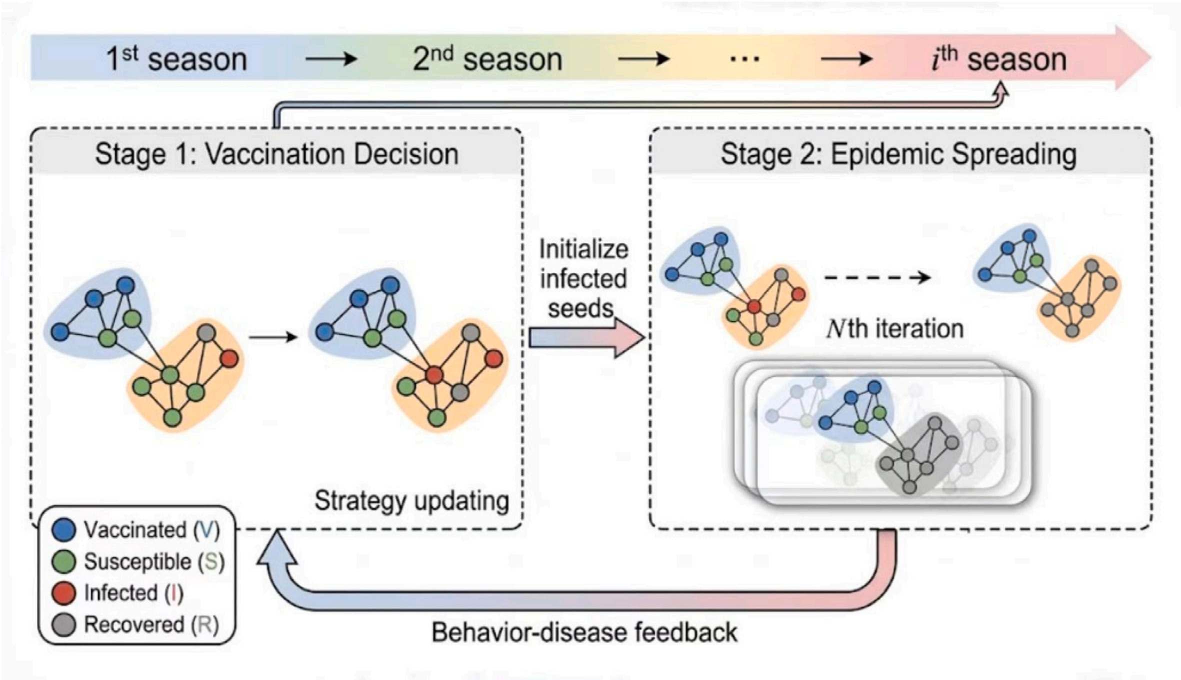

Fig. 1. A schematic diagram of the co-evolutionary framework of vaccination behavior and epidemic spread. The top timeline shows the seasonal evolution, where each season consists of two stages: vaccination decision and epidemic spreading. Individuals initially experience epidemic dynamics under a fixed vaccination configuration, then allocate benefits based on vaccination and infection outcomes. Strategies are then updated through a benefit-driven mimicry process, and the updated strategies determine the vaccination status for the next epidemic season. Node colors indicate individual states: vaccinated (V, blue), susceptible (S, green), infected (I, red), and recovered (R, gray). The bottom arrows indicate the feedback loop between epidemic outcomes and subsequent behavioral adaptation across seasons.

are assigned to state V, while all other individuals are initialized as susceptible. A fixed number $I_0 = 10$ of individuals are randomly selected as initial infected seeds. Infection occurs along network edges, with each susceptible node becoming infected at a rate proportional to the number of its infected neighbors (i.e., γ per infected neighbor), while recovery occurs independently at rate μ. The process continues until no infected individuals remain or a maximum simulation time is reached.

To model community-level lockdown, we introduce a transmission suppression mechanism acting on inter-community contacts. Specifically, transmission between individuals belonging to different communities occurs at a reduced rate $\gamma(1-p)$, where $p \in [0,1]$ represents the strength of community lockdown. When $p = 0$, no lockdown is applied, while $p = 1$ corresponds to a complete suppression of inter-community transmission. Transmission within the same community remains unchanged. We model community-level lockdown as a reduction in inter-community transmission rates by a factor $(1-p)$, which provides a minimal and interpretable representation of decreased effective contact intensity across communities. This formulation captures the impact of mobility restrictions and reduced cross-community interactions without altering the underlying network topology.

2.3. Simulation settings

To investigate the impact of community lockdown on epidemic spreading and the vaccination dilemma, we perform numerical simulations on hyperbolic networks. Unless otherwise specified, the following parameter settings are used throughout the study. The network size is set to $N = 5000$ with an average degree $\langle k \rangle = 6$. The transmission rate is $\gamma = 0.51$, and the recovery rate is $\mu = 1/3$. The initial number of infected individuals is $I_0 = 10$. For the visualization results shown in Figs. 4 and 5, a smaller network size ($N = 3000$) is used to improve the readability of temporal and spatial patterns. To ensure that the system reaches a steady state, the simulation is run for 3000 epidemic seasons. The average values over the last 1000 seasons are taken as the final vaccination coverage and epidemic size. In addition, more than 20 independent realizations are performed for each set of parameters to reduce statistical fluctuations.

3. Result

We first examine how vaccination coverage and epidemic size depend on the vaccination cost under different levels of community lockdown. As shown in Fig. 2, increasing the vaccination cost can be associated with a decline in vaccination coverage and a corresponding increase in epidemic size, which is consistent with classical voluntary vaccination dynamics. However, the effect

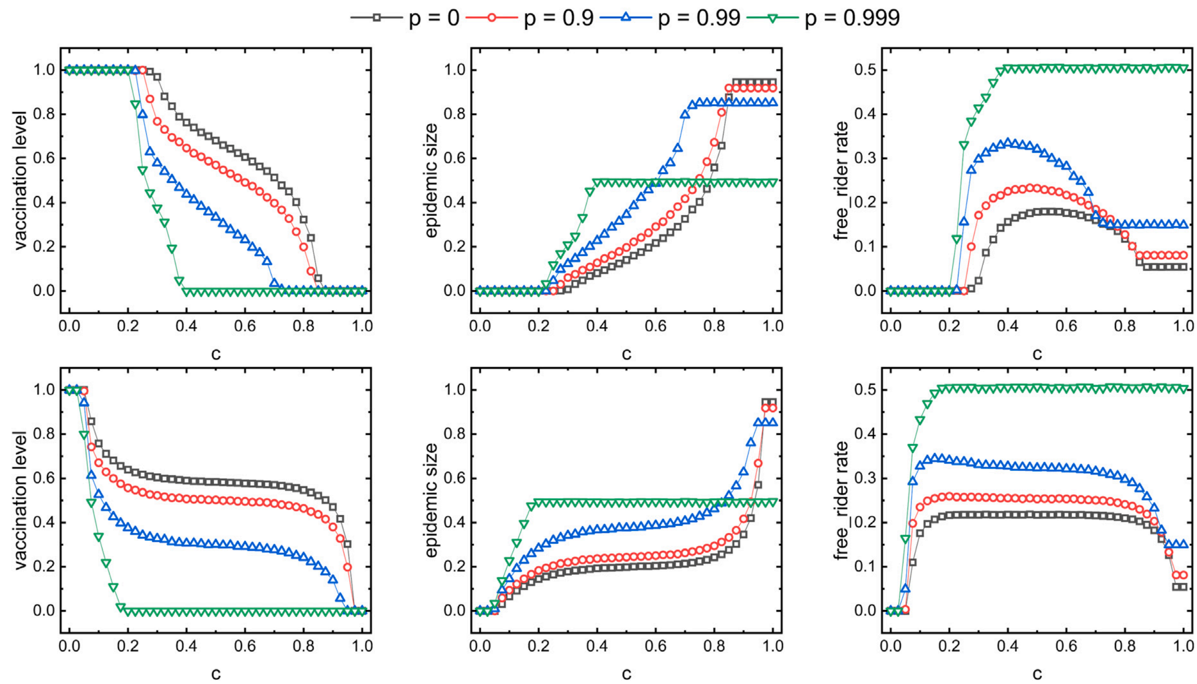

Fig. 2. Vaccine coverage, outbreak size, and free-rider ratio vary with vaccination costs under different levels of community lockdown. The left column shows the steady-state average vaccine coverage, the middle column shows the final outbreak size, and the right column shows the proportion of free-riders. The horizontal axis represents the relative vaccination cost c. The upper row corresponds to selection intensity $\beta = 1$, whereas the lower row corresponds to selection intensity $\beta = 10$. Different symbols and colors denote different strengths of community isolation: $p = 0$ (no isolation), $p = 0.9$, $p = 0.99$, and $p = 0.999$. The figure illustrates how the effectiveness of lockdown depends on vaccination cost and how behavioral responses influence epidemic outcomes. Main parameters are: network size $N = 5000$, average degree $\langle k \rangle = 6$, transmission rate $\gamma = 0.51$, recovery rate $\mu = 1/3$, and initial number of infected individuals $I_0 = 10$.

of community lockdown varies with the vaccination cost, and the curves exhibit qualitatively different patterns in different cost regimes.

When the vaccination cost is low, vaccination coverage remains close to full adoption across all lockdown levels, and the epidemic size stays at a very low level. In this regime, individuals have strong incentives to vaccinate, so the population is effectively protected by widespread immunization and differences in lockdown intensity produce almost no visible effect on either vaccination coverage or epidemic size. As the vaccination cost increases to an intermediate range, the vaccination curves begin to separate clearly under different lockdown levels. Stronger lockdown is observed to coincide with a faster decline in vaccination coverage, suggesting that reduced cross-community interactions lower overall infection exposure. Under the present evolutionary updating framework, this reduced exposure subsequently weakens the incentive to vaccinate. At the same time, the epidemic-size curves do not decrease proportionally with increasing lockdown intensity; instead, they may remain comparable to, or even exceed, those in the absence of lockdown. This reveals a counterintuitive regime in which the direct transmission-suppressing effect of lockdown is partially offset by the decline in vaccination coverage induced by free-riding behavior. When the vaccination cost becomes high, vaccination coverage approaches zero under all lockdown levels, and the epidemic size rises sharply. In this regime, behavioral adaptation through vaccination is effectively absent, so epidemic control relies almost entirely on lockdown. Increasing lockdown intensity then significantly reduces epidemic size, showing that lockdown regains its effectiveness as a transmission-limiting mechanism. Even so, under extremely strong lockdown (e.g., $p = 0.999$), a considerable fraction of the population remains infected, indicating that lockdown alone cannot fully suppress the outbreak.

Since infection size alone does not fully capture the combined effects of epidemic spreading and vaccination behavior, we next consider the overall social cost by accounting for both vaccination expenditure and infection-related losses. The average social cost is defined as the average cost paid by all individuals in the entire population after the epidemic has reached a steady state. As shown in Fig. 3, the average social cost increases monotonically with vaccination cost under all lockdown intensities, but the detailed shapes of the curves differ substantially across regimes. When vaccination cost is low ($c \lesssim 0.4$), the social-cost curves under different lockdown levels nearly overlap and remain at a low level, since vaccination coverage is high and epidemic spreading is effectively suppressed. In this regime, the total cost is dominated mainly by vaccination expenditure, and the influence of lockdown is negligible. As c increases into the intermediate range, a clear separation between curves emerges, together with an approximate transition point around $c \approx 0.5$. Below this threshold, stronger lockdown leads to higher social cost. This is because vaccination remains widespread, and additional restrictions mainly reduce system efficiency without significantly lowering infection burden.

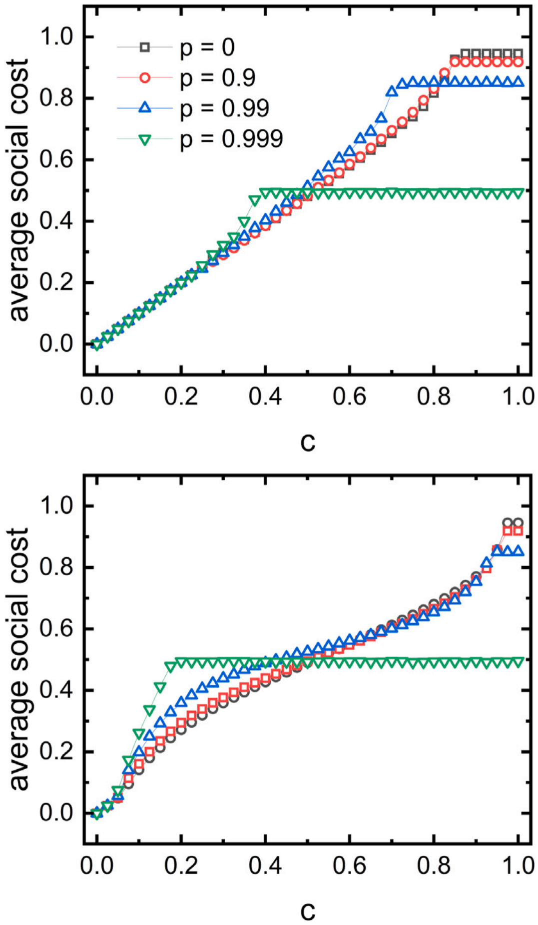

Fig. 3. Average social cost as a function of vaccination cost under different levels of community lockdown. The horizontal axis represents the relative vaccination cost c, and the vertical axis denotes the average social cost. The social cost accounts for both vaccination cost and infection loss. The upper row corresponds to selection intensity $\beta = 1$, whereas the lower row corresponds to selection intensity $\beta = 10$. Different curves correspond to different lockdown intensities: $p = 0$ (no lockdown), $p = 0.9$, $p = 0.99$, and $p = 0.999$. Other parameters are set as $N = 5000$, $\langle k \rangle = 6$, $\gamma = 0.51$, $\mu = 1/3$, and $I_0 = 10$.

Above this threshold, however, the trend reverses: stronger lockdown results in lower social cost. In this regime, vaccination uptake declines substantially, and reducing transmission through lockdown becomes more effective in limiting infection-related losses. When vaccination cost becomes high ($c \gtrsim 0.8$), vaccination coverage is negligible and social cost is dominated by infection-related losses. In the absence of effective lockdown, widespread outbreaks cause the total cost to rise rapidly. Under stronger lockdown, the growth of social cost is significantly slowed, although large-scale infection still persists.

To further explore the underlying mechanism, we examine the temporal evolution of the system over successive epidemic seasons, as shown in Fig. 4. In this figure, the left and right columns correspond to the cases without lockdown ($p = 0$) and with strong lockdown ($p = 0.999$), respectively, while the top and bottom rows represent different selection intensities ($\beta = 1$ and $\beta = 10$). Each time step represents one epidemic season followed by strategy updating.

Due to the high vaccination cost, the vaccination coverage rapidly approaches zero in all cases. This effectively removes the influence of vaccination behavior, allowing us to isolate the direct impact of lockdown on epidemic spreading. Without lockdown, the system rapidly evolves into an infection-dominated state, where the disease spreads globally and reaches a relatively stable level with small fluctuations. This indicates that, in the absence of constraints on inter-community interactions, epidemic spreading organizes into a synchronized outbreak across the entire network. With strong lockdown, although the average infection level is reduced, the temporal dynamics become highly irregular, exhibiting persistent large-amplitude fluctuations. Instead of converging to a steady state, the system remains dynamically active over time. This behavior arises from the spatial fragmentation induced by lockdown: when cross-community transmission is suppressed, epidemic spreading is confined within individual communities, leading to asynchronous local outbreaks. The aggregate dynamics therefore reflect the superposition of multiple desynchronized processes, resulting in sustained temporal variability. These temporal patterns remain qualitatively similar for $\beta = 1$ and $\beta = 10$, indicating that the high-amplitude fluctuations induced by community lockdown are robust rather than incidental. This observation motivates a further examination from a microscopic perspective.

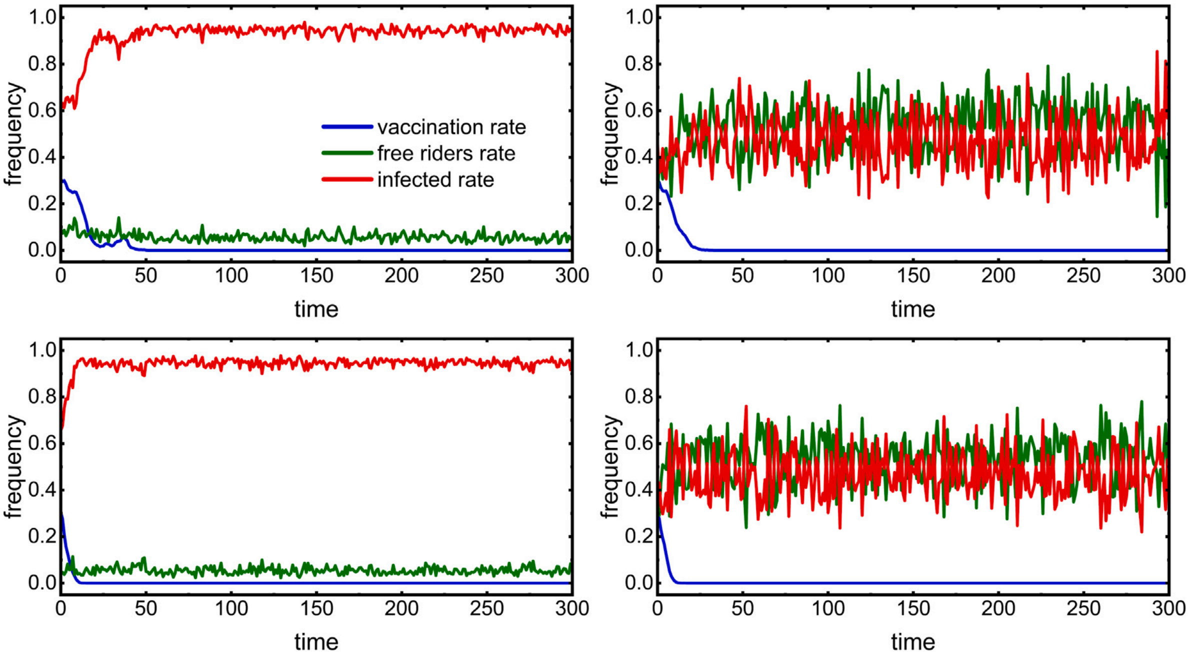

Fig. 4. The temporal evolution of vaccination behavior and epidemic transmission. The blue curve represents the proportion of vaccinated individuals; the green curve indicates the proportion of unvaccinated but uninfected "free-riders"; and the red curve denotes the proportion of infected individuals. The left column illustrates the scenario without community isolation ($p = 0$), while the right column corresponds to the scenario with strong community isolation ($p = 0.999$). The horizontal axis corresponds to the Monte Carlo evolutionary cycles; The upper row corresponds to selection intensity $\beta = 1$, whereas the lower row corresponds to selection intensity $\beta = 10$. Main parameters are: network size $N = 3000$, average degree $\langle k \rangle = 6$, transmission rate $\gamma = 0.51$, recovery rate $\mu = 1/3$, $c = 0.9$ and the initial infected individuals are confined to designated communities.

Fig. 5 shows the spatial evolution of node states at different stages of the epidemic process. The top row corresponds to the case without lockdown, while the bottom row represents strong community lockdown. The system is simulated under a high vaccination-cost regime, in which vaccination coverage quickly approaches zero. This setup effectively removes the influence of vaccination behavior, allowing the impact of community lockdown on epidemic spreading to be observed more clearly. At the initial stage, a small number of infected individuals ($I_0 = 10$) are randomly distributed across the network. For visualization purposes, vaccinated individuals are initially placed in a few selected communities (blue nodes), which helps highlight their spatial evolution but does not affect the overall dynamics. Without lockdown, infections rapidly cross community boundaries and spread across the entire network. As the process evolves, the infected nodes become more uniformly distributed in space, and most communities are eventually involved in the outbreak. Although vaccinated nodes may transiently extend into neighboring regions in the early stage, they gradually disappear as vaccination becomes unfavorable and free-riding dominates. The final spatial pattern is therefore characterized by a largely homogeneous distribution of infected nodes. With strong lockdown, the spreading pattern is fundamentally altered. Transmission is largely confined within individual communities, and the epidemic remains localized within a subset of regions at each stage. Instead of expanding uniformly, active outbreak regions shift between communities over time, while other communities remain weakly affected or nearly disease-free. This persistent spatial heterogeneity reflects the fragmentation of transmission pathways induced by lockdown. These spatial patterns provide a direct microscopic explanation for the temporal dynamics observed in Fig. 4. The irregular fluctuations at the system level arise from the superposition of multiple asynchronous local outbreaks occurring in different communities.

Finally, we relaxed the idealized assumption of perfect vaccine-induced protection, since real-world vaccine efficacy is often incomplete, particularly in the presence of viral mutation and immune escape. To account for this, we introduced an imperfect-vaccine scenario with a baseline vaccine efficacy of $E_v = 0.8$, meaning that vaccination reduces an individual's susceptibility to infection by 80% rather than conferring complete immunity. Under this setting, vaccinated individuals may still experience breakthrough infections and consequently bear both the vaccination cost and the losses associated with infection. As shown in Fig. 6, compared with the perfect-vaccine case, vaccination coverage declines more rapidly as vaccination costs increase and collapses at a substantially lower threshold ($c \approx 0.2$), reflecting the reduced expected payoff of vaccination under imperfect protection. More importantly, the counterintuitive "lockdown paradox" observed in Fig. 2 disappears entirely: stronger lockdown measures consistently suppress epidemic prevalence across the full range of vaccination costs.

The contrast between the perfect and imperfect vaccine scenarios helps clarify the mechanism underlying this paradox. Under perfect protection, vaccination effectively eliminates infection risk and therefore promotes free-riding behavior, making vaccination

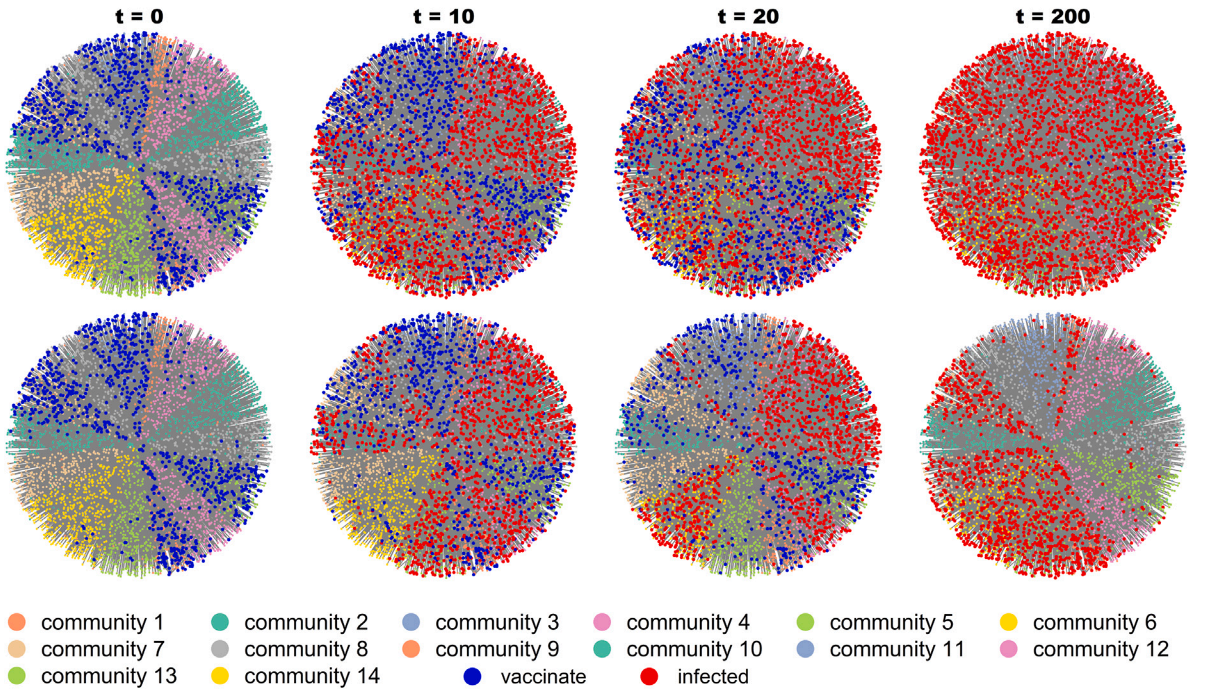

Fig. 5. Spatiotemporal pattern formation of vaccination behavior and epidemic spreading on the hyperbolic network. Different background colors indicate different community structures. Blue nodes represent vaccinated individuals, while red nodes denote unvaccinated individuals who have been infected, including both infectious and recovered states. From left to right, the panels correspond to the system states at $t = 0$, $t = 10$, $t = 20$, and $t = 200$, respectively. The upper row shows the case without community isolation ($p = 0$), whereas the lower row corresponds to strong community isolation ($p = 0.999$). Main parameters are: network size $N = 3000$, average degree $\langle k \rangle = 6$, transmission rate $\gamma = 0.51$, recovery rate $\mu = 1/3$, $c = 0.9$, $\beta = 1$ and the initial infected individuals are confined to designated communities.

decisions highly sensitive to perceived epidemic risk. As lockdown measures reduce transmission, individuals become less motivated to vaccinate, which can partially offset the epidemiological benefits of lockdown and even produce counterintuitive system-level outcomes. In contrast, when vaccine efficacy is imperfect, vaccinated individuals are still partially exposed to infection risk, which to some extent weakens the motivation for free-riding and reduces the dynamic coupling strength between perceived risk and vaccination rates. Therefore, epidemic dynamics are more directly influenced by the suppressive effect of lockdown interventions. In this sense, the disappearance of the paradox under imperfect vaccination does not imply a reduced importance of behavioral feedback; rather, it further emphasizes that the impact of non-pharmaceutical interventions critically depends on the coupling between epidemic dynamics and adaptive human behavior.

4. Discussion

In this study, we investigated the coevolution of epidemic spreading and vaccination behavior under community lockdown on hyperbolic networks. By combining geometric network structure, epidemic dynamics, and evolutionary vaccination decisions within a unified framework, we examined how transmission processes and individual behavior jointly shape epidemic outcomes.

Our results show that the effect of community lockdown depends strongly on vaccination cost. When vaccination is inexpensive and widely adopted, lockdown contributes little because epidemic spread is already strongly suppressed. At intermediate vaccination costs, however, lockdown reduces overall infection exposure, which, within the evolutionary game framework, diminishes the payoff-driven incentive to vaccinate. This behavioral response can generate counterintuitive outcomes, including larger outbreaks despite reduced transmission. When vaccination becomes prohibitively costly, lockdown acts as the primary control mechanism and can substantially reduce epidemic size, although it cannot eliminate transmission entirely. These findings indicate that the role of lockdown is not fixed, but emerges from its interplay with behavioral adaptation.

To place these findings into a broader network context, it is important to note that empirical social networks are known to exhibit pronounced community structure [5], which plays a crucial and often nontrivial role in shaping epidemic spreading dynamics [47–49]. In particular, the interplay between densely connected local neighborhoods and sparser long-range connections, often associated with human mobility patterns, has been shown to critically influence both the speed and extent of disease propagation. Short-range interactions tend to sustain local outbreaks, while long-range ties facilitate global spreading by bridging otherwise weakly connected communities [50]. These structural features also have important implications for epidemic control, as they determine how interventions targeting mobility or contact patterns can mitigate large-scale outbreaks [51]. In this context,

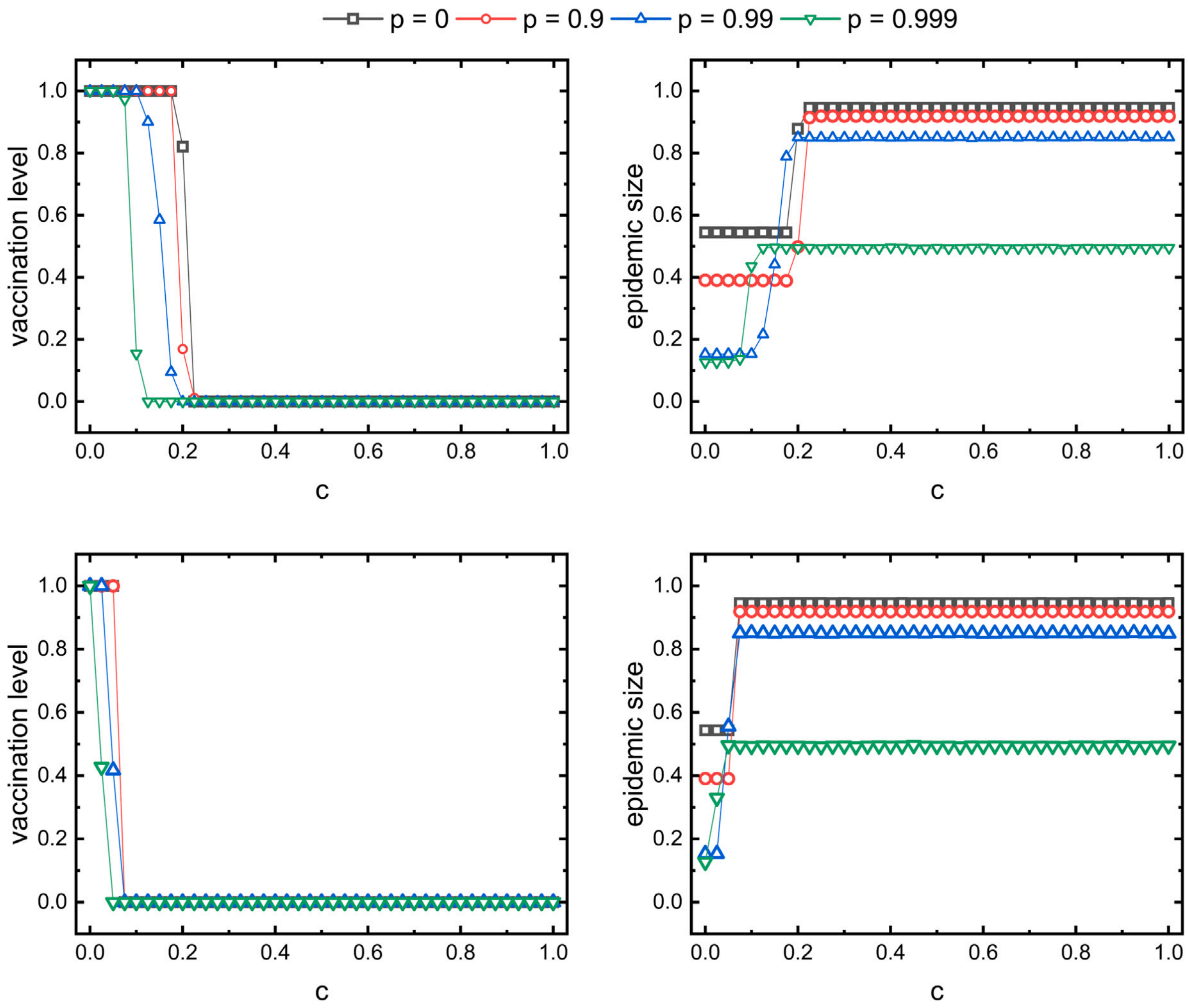

Fig. 6. Vaccination coverage and epidemic size versus the relative vaccination cost c under different levels of community lockdown in the imperfect-vaccine scenario. The left column shows the steady-state vaccination coverage, and the right column shows the final epidemic size. The upper row corresponds to selection intensity $\beta = 1$, while the lower row corresponds to $\beta = 10$. Different symbols and colors represent different levels of community lockdown: $p = 0$ (no isolation), $p = 0.9$, $p = 0.99$, and $p = 0.999$. Parameters are set to $N = 5000$, $\langle k \rangle = 6$, $\gamma = 0.51$, $\mu = 1/3$, $E_v = 0.8$, and $I_0 = 10$.

community-level interventions, including mobility restrictions and reduced inter-community contacts, have been widely studied as key non-pharmaceutical strategies to suppress epidemic spreading [7,51–53]. Empirical and modeling studies have demonstrated that limiting cross-community interactions can effectively reduce transmission, particularly in the early stages of an outbreak. However, previous work on hyperbolic networks has shown that such structural interventions alone may not suffice to prevent large-scale spreading, even under strong reductions in inter-community transmission [30]. This suggests that the effectiveness of community-level lockdown is inherently constrained by the underlying network structure.

Beyond purely structural considerations, it is increasingly recognized that the impact of epidemic interventions is strongly context-dependent and may be further shaped by adaptive human behavior. In particular, fluctuations in local infection exposure can dynamically alter the payoff landscape of individuals, thereby modifying the collective response to interventions. Incorporating such behavioral feedback is therefore essential for a more complete understanding of how transmission dynamics and control measures interact. It is worth noting that Fenichel et al. showed that incorporating adaptive human behavior can substantially alter the predicted epidemic dynamics [21]. Their study demonstrated that controlling epidemics solely by reducing contact rates may generate economic losses exceeding the burden of the epidemic itself, and that policies maximizing infection reduction do not necessarily maximize overall social welfare. Consistent with this perspective, our study further considers the dynamic interplay among epidemic spreading, vaccination feedback, and social interventions within a more realistic co-evolutionary framework. We find that, under the assumption of perfect vaccine-induced protection, individuals may exhibit stronger free-riding behavior after weighing vaccination costs against perceived infection risk. Consequently, as community lockdown measures reduce transmission risk, vaccination incentives may also decline, partially offsetting the epidemiological benefits of lockdown and even leading to larger-than-expected epidemic outbreaks. In this sense, our results further highlight the importance of incorporating adaptive behavioral responses when evaluating the effectiveness of non-pharmaceutical interventions.

While our framework reveals the fundamental mechanisms of the lockdown-vaccination trade-off, it relies on some simplifying assumptions to explicitly isolate the core mechanisms of the behavior-disease feedback. First, our primary analysis assumes perfect vaccine-induced protection. Although such an idealized condition is difficult to achieve in real-world settings, it provides a limiting case in which the negative impact of behavioral feedback on the effectiveness of community lockdowns can be clearly identified. To examine whether this mechanism persists under more realistic vaccine conditions, we further considered an imperfect-vaccine scenario. This extension changes not only the direct level of vaccine protection, but also the payoff structure underlying vaccination decisions: vaccinated individuals may still become infected and therefore bear both vaccination costs and infection-related losses. From the perspective of social learning, this reduces the relative advantage of vaccination and weakens individuals' responsiveness to changes in perceived infection risk. As the coupling between behavioral adaptation and epidemic spreading becomes weaker, the system gradually shifts from a strongly co-evolutionary regime toward dynamics more strongly governed by transmission processes, under which conventional interventions such as community lockdowns recover their expected epidemic-control effectiveness. Nevertheless, this comparison further highlights that adaptive behavioral feedback can fundamentally reshape epidemic outcomes and the effectiveness of public-health interventions. Second, our model represents community-level lockdown as a homogeneous reduction of inter-community transmission rates. While this simplified formulation allows for a clear and controlled investigation of the interplay between network structure and behavioral adaptation, it does not capture more complex forms of intervention, such as heterogeneous mobility reductions, targeted isolation strategies, or dynamic rewiring of contact patterns. Exploring these extensions, particularly how imperfect immunity interacts with targeted mobility restrictions over multiple seasons, would provide a more detailed representation of real-world scenarios and represents an important direction for future work. From a broader perspective, our results suggest that epidemic control strategies based solely on transmission reduction may produce unintended consequences if behavioral feedback is neglected. Effective intervention policies should therefore consider not only their direct epidemiological impact, but also their influence on individual decision-making and risk perception.

From a dynamical perspective, lockdown also qualitatively reorganizes the spreading process. Instead of synchronized global outbreaks, the system exhibits fragmented and asynchronous local transmission waves, which produce persistent temporal fluctuations. This structural fragmentation offers a microscopic explanation for the macroscopic variability observed in the epidemic dynamics.

By further incorporating a cost-based evaluation, we show that the influence of lockdown extends beyond epidemic size to the overall social cost. In particular, a crossover appears at intermediate vaccination costs, where the relative benefit of lockdown changes. This marks a shift from vaccination-dominated protection to transmission-limited control and underscores the need to account for epidemiological and behavioral factors simultaneously.

These results have several broader implications. First, voluntary vaccination alone may produce suboptimal outcomes because individuals can free-ride on the protection provided by others. Second, although strong lockdown measures can reduce epidemic spread, their effect is inherently limited and may be difficult to sustain in practice. Most importantly, excessive reliance on lockdown may weaken vaccination incentives, thereby offsetting part of its epidemiological benefit. Effective epidemic control therefore requires a balance between mobility restrictions and policies that preserve or strengthen vaccine uptake.

Overall, our findings highlight the central role of behavioral feedback in epidemic dynamics and show that successful intervention strategies must address both transmission pathways and individual decision-making. Future work could extend this framework by incorporating more realistic behavioral responses, heterogeneous risk perception, or adaptive policy mechanisms.

CRediT authorship contribution statement

Shaojun Dang: Funding acquisition, Formal analysis, Conceptualization. **Xiaoqian Zhao:** Writing – original draft, Investigation. **Marko Gosak:** Writing – review & editing, Conceptualization. **Kaipeng Hu:** Software, Methodology, Formal analysis. **Matjaž Perc:** Writing – review & editing, Conceptualization.

Declaration of competing interest

The authors declare that they have no known competing financial interests or personal relationships that could have appeared to influence the work reported in this paper.

Acknowledgments

S. Dang was supported by the Scientific Research Fund Project of the Yunnan Provincial Education Department (Grant Nos. 2026Y0838, 2026Y0839, 2026Y0834). K. Hu was supported by the Yunnan Fundamental Research Projects (Grant Nos. 202401AU070100, 202501AT070450). M. Perc was supported by the Slovenian Research and Innovation Agency (Grant No. P1-0403). M. Gosak was supported by the Slovenian Research and Innovation Agency (Grant Nos. SN-ZRD/22-27/0552, P3-0396, and I0-0029).

Data availability

Data will be made available on request.

References

[1] Albert-László Barabási, Réka Albert, Emergence of scaling in random networks, Science 286 (5439) (1999) 509–512.
[2] Duncan J. Watts, Steven H. Strogatz, Collective dynamics of 'small-world' networks, Nature 393 (6684) (1998) 440–442.
[3] Mark E.J. Newman, The structure and function of complex networks, SIAM Rev. 45 (2) (2003) 167–256.
[4] Santo Fortunato, Community detection in graphs, Phys. Rep. 486 (3–5) (2010) 75–174.
[5] Michelle Girvan, Mark E.J. Newman, Community structure in social and biological networks, Proc. Natl. Acad. Sci. USA 99 (12) (2002) 7821–7826.
[6] Matjaž Perc, Attila Szolnoki, Social diversity and promotion of cooperation in the spatial prisoner's dilemma game, Phys. Rev. E 77 (1) (2008) 011904.
[7] Marcel Salathé, James H. Jones, Dynamics and control of diseases in networks with community structure, PLoS Comput. Biol. 6 (4) (2010) e1000736.
[8] Quantong Guo, Yanjun Lei, Chengyi Xia, Lu Guo, Xin Jiang, Zhiming Zheng, The role of node heterogeneity in the coupled spreading of epidemics and awareness, PLoS One 11 (8) (2016) e0161037.
[9] Bnaya Gross, Shlomo Havlin, Epidemic spreading and control strategies in spatial modular network, Appl. Netw. Sci. 5 (1) (2020) 95.
[10] Nicholas A. Christakis, James H. Fowler, Connected: The Surprising Power of Our Social Networks and How They Shape Our Lives, Hachette UK, 2009.
[11] Zhen Wang, Attila Szolnoki, Matjaž Perc, Interdependent network reciprocity in evolutionary games, Sci. Rep. 3 (1) (2013) 1183.
[12] Timothy C. Reluga, Game theory of social distancing in response to an epidemic, PLoS Comput. Biol. 6 (5) (2010) e1000793.
[13] Jay J Van Bavel, Katherine Baicker, Paulo S Boggio, Valerio Capraro, Aleksandra Cichocka, Mina Cikara, Molly J Crockett, Alia J Crum, Karen M Douglas, James N Druckman, et al., Using social and behavioural science to support COVID-19 pandemic response, Nat. Hum. Behav. 4 (5) (2020) 460–471.
[14] Chris T. Bauch, David J.D. Earn, Vaccination and the theory of games, Proc. Natl. Acad. Sci. USA 101 (36) (2004) 13391–13394.
[15] Matjaž Perc, Jillian J Jordan, David G Rand, Zhen Wang, Stefano Boccaletti, Attila Szolnoki, Statistical physics of human cooperation, Phys. Rep. 687 (2017) 1–51.
[16] Attila Szolnoki, Matjaž Perc, Coevolutionary success-driven multigames, EPL 108 (2) (2014) 28004.
[17] Matjaž Perc, Jesús Gómez-Gardenes, Attila Szolnoki, Luis M Floría, Yamir Moreno, Evolutionary dynamics of group interactions on structured populations: a review, J. R. Soc. Interface 10 (80) (2013).
[18] Stephan Eubank, I Eckstrand, B Lewis, Srinivasan Venkatramanan, Madhav Marathe, CL Barrett, Commentary on ferguson, et al.,"impact of non-pharmaceutical interventions (NPIs) to reduce COVID-19 mortality and healthcare demand", Bull. Math. Biol. 82 (4) (2020) 52.
[19] Seth Flaxman, Swapnil Mishra, Axel Gandy, H Juliette T Unwin, Thomas A Mellan, Helen Coupland, Charles Whittaker, Harrison Zhu, Tresnia Berah, Jeffrey W Eaton, et al., Estimating the effects of non-pharmaceutical interventions on COVID-19 in europe, Nature 584 (7820) (2020) 257–261.
[20] Moritz UG Kraemer, Chia-Hung Yang, Bernardo Gutierrez, Chieh-Hsi Wu, Brennan Klein, David M Pigott, Open COVID-19 Data Working Group†, Louis Du Plessis, Nuno R Faria, Ruoran Li, et al., The effect of human mobility and control measures on the COVID-19 epidemic in China, Science 368 (6490) (2020) 493–497.
[21] Eli P Fenichel, Carlos Castillo-Chavez, M Graziano Ceddia, Gerardo Chowell, Paula A Gonzalez Parra, Graham J Hickling, Garth Holloway, Richard Horan, Benjamin Morin, Charles Perrings, et al., Adaptive human behavior in epidemiological models, Proc. Natl. Acad. Sci. USA 108 (15) (2011) 6306–6311.
[22] Chris T. Bauch, Imitation dynamics predict vaccinating behaviour, Proc. R. Soc. B 272 (1573) (2005) 1669–1675.
[23] Feng Fu, Daniel I. Rosenbloom, Long Wang, Martin A. Nowak, Imitation dynamics of vaccination behaviour on social networks, Proc. R. Soc. B 278 (1702) (2011) 42–49.
[24] Zhen Wang, Chris T Bauch, Samit Bhattacharyya, Alberto d'Onofrio, Piero Manfredi, Matjaž Perc, Nicola Perra, Marcel Salathé, Dawei Zhao, Statistical physics of vaccination, Phys. Rep. 664 (2016) 1–113.
[25] Lang Cao, Xun Li, Impacts of evolutionary vaccine games on the spread of infectious diseases, in: 2016 35th Chinese Control Conference, CCC, IEEE, 2016, pp. 10357–10362.
[26] Xinyu Wang, Danyang Jia, Shupeng Gao, Chengyi Xia, Xuelong Li, Zhen Wang, Vaccination behavior by coupling the epidemic spreading with the human decision under the game theory, Appl. Math. Comput. 380 (2020) 125232.
[27] Haifeng Zhang, Feng Fu, Wenyao Zhang, Binghong Wang, Rational behavior is a 'double-edged sword'when considering voluntary vaccination, Phys. A 391 (20) (2012) 4807–4815.
[28] Cornelia Betsch, Robert Böhm, Lars Korn, Inviting free-riders or appealing to prosocial behavior? game-theoretical reflections on communicating herd immunity in vaccine advocacy, Health Psychol. 32 (9) (2013) 978.
[29] Romualdo Pastor-Satorras, Alessandro Vespignani, Epidemic spreading in scale-free networks, Phys. Rev. Lett. 86 (14) (2001) 3200.
[30] Marko Gosak, Maja Duh, Rene Markovič, MatjaŽ Perc, Community lockdowns in social networks hardly mitigate epidemic spreading, New J. Phys. 23 (4) (2021) 043039.
[31] Dmitri Krioukov, Fragkiskos Papadopoulos, Maksim Kitsak, Amin Vahdat, Marián Boguná, Hyperbolic geometry of complex networks, Phys. Rev. E 82 (3) (2010) 036106.
[32] Maja Duh, Marko Gosak, Matjaž Perc, Public goods games on random hyperbolic graphs with mixing, Chaos Solitons Fractals 144 (2021) 110720.
[33] Odo Diekmann, Johan Andre Peter Heesterbeek, Mathematical Epidemiology of Infectious Diseases: Model Building, Analysis and Interpretation, vol. 5, John Wiley & Sons, 2000.
[34] Marián Boguná, Fragkiskos Papadopoulos, Dmitri Krioukov, Sustaining the internet with hyperbolic mapping, Nat. Commun. 1 (1) (2010) 62.
[35] Konstantin Zuev, Marián Boguñá, Ginestra Bianconi, Dmitri Krioukov, Emergence of soft communities from geometric preferential attachment, Sci. Rep. 5 (1) (2015) 9421.
[36] Maja Duh, Marko Gosak, Matjaž Perc, Unexpected paths to cooperation on tied hyperbolic networks, EPL 142 (6) (2023) 62002.
[37] Mark E.J. Newman, Michelle Girvan, Finding and evaluating community structure in networks, Phys. Rev. E 69 (2) (2004) 026113.
[38] Mark D. Humphries, Kevin Gurney, Network 'small-world-ness': a quantitative method for determining canonical network equivalence, PLoS One 3 (4) (2008) e0002051.
[39] Kaj-Kolja Kleineberg, Metric clusters in evolutionary games on scale-free networks, Nat. Commun. 8 (1) (2017) 1888.
[40] Marko Gosak, Moritz UG Kraemer, Heinrich H Nax, Matjaž Perc, Bary SR Pradelski, Endogenous social distancing and its underappreciated impact on the epidemic curve, Sci. Rep. 11 (1) (2021) 3093.
[41] Rene Markovič, Marko Šterk, Marko Marhl, Matjaž Perc, Marko Gosak, Socio-demographic and health factors drive the epidemic progression and should guide vaccination strategies for best COVID-19 containment, Results Phys. 26 (2021) 104433.
[42] Lawrence E. Blume, The statistical mechanics of strategic interaction, Games Econom. Behav. 5 (3) (1993) 387–424.
[43] György Szabó, Csaba Tőke, Evolutionary prisoner's dilemma game on a square lattice, Phys. Rev. E 58 (1) (1998) 69.
[44] Arne Traulsen, Jorge M. Pacheco, Martin A. Nowak, Pairwise comparison and selection temperature in evolutionary game dynamics, J. Theoret. Biol. 246 (3) (2007) 522–529.

[45] Daniel T. Gillespie, Exact stochastic simulation of coupled chemical reactions, J. Phys. Chem. 81 (25) (1977) 2340–2361.
[46] Naoki Masuda, Christian L. Vestergaard, Gillespie Algorithms for Stochastic Multiagent Dynamics in Populations and Networks, Cambridge University Press, 2023.
[47] Zonghua Liu, Bambi Hu, Epidemic spreading in community networks, EPL 72 (2) (2005) 315–321.
[48] Clara Stegehuis, Remco Van Der Hofstad, Johan SH Van Leeuwaarden, Epidemic spreading on complex networks with community structures, Sci. Rep. 6 (1) (2016) 29748.
[49] Lucas D. Valdez, Lidia A. Braunstein, Shlomo Havlin, Epidemic spreading on modular networks: The fear to declare a pandemic, Phys. Rev. E 101 (3) (2020) 032309.
[50] Jianhong Mou, Suoyi Tan, Juanjuan Zhang, Bin Sai, Mengning Wang, Bitao Dai, Bo-Wen Ming, Shan Liu, Zhen Jin, Guiquan Sun, et al., Strong long ties facilitate epidemic containment on mobility networks, PNAS Nexus 3 (11) (2024) pgae515.
[51] Xin Lu, Jiawei Feng, Shengjie Lai, Petter Holme, Shuo Liu, Zhanwei Du, Xiaoqian Yuan, Siqing Wang, Yunxuan Li, Xiaoyu Zhang, et al., Human mobility in epidemic modeling, Phys. Rep. 1157 (2026) 1–45.
[52] Ta-Chien Chan, Ching-Chi Chou, Yi-Chi Chu, Jia-Hong Tang, Li-Chi Chen, Hsien-Ho Lin, Kevin J Chen, Ran-Chou Chen, Effectiveness of controlling COVID-19 epidemic by implementing soft lockdown policy and extensive community screening in Taiwan, Sci. Rep. 12 (1) (2022) 12053.
[53] Per Block, Marion Hoffman, Isabel J Raabe, Jennifer Beam Dowd, Charles Rahal, Ridhi Kashyap, Melinda C Mills, Social network-based distancing strategies to flatten the COVID-19 curve in a post-lockdown world, Nat. Hum. Behav. 4 (6) (2020) 588–596.